A DIFFERENTIAL EVOLUTION-BASED APPROACH FOR GEOMETRICALLY NONLINEAR ANALYSIS OF TRUSS STRUCTURES

MAI TIEN HAU

[1] *Faculty of Mechanical Engineering, Industrial University of Ho Chi Minh City, Ho Chi Minh City*

Corresponding author: maitienhau@iuh.edu.vn

DOIs: https://www.doi.org/10.46242/jstiuh.v81i3.6014

Abstract. This study presents a Differential Evolution (DE)-based energy-minimization framework for geometrically nonlinear truss analysis. The equilibrium configuration is determined by minimizing the Total Potential Energy (TPE) using DE, avoiding stiffness updates and incremental–iterative solvers. The DE algorithm is derivative-free and parameter-light, offering robust global search in nonlinear energy landscapes. In this framework, the displacement field is treated as the design variables, and the nonlinear structural responses are obtained through direct minimization of the energy functional without computing tangent stiffness matrices or evaluating derivatives. The performance of the proposed framework is evaluated through several benchmark geometrically nonlinear truss examples, and the obtained solutions are compared with reference solutions and other metaheuristic optimizers such as Teaching-Learning-Based Optimization (TLBO), Firefly Algorithm (FA), and Backtracking Search Algorithm (BSA). The results demonstrate that the proposed method accurately captures the equilibrium state of the structure.

Keywords. Nonlinear analysis; Truss structure; Geometric nonlinearity; Differential evolution

1 INTRODUCTION

The mechanical response of most structures is inherently nonlinear [1]. Such geometric and material nonlinearities complicate the design process and require advanced analytical techniques for accurate characterization of structural behavior [2]. Over the past few decades, many algorithms have been developed to address nonlinear structural problems, which can generally be categorized into two main groups. The first category, referred to as the stiffness-based approach based on the Finite Element Method (FEM), adopts incremental–iterative schemes, such as the quasi–Newton, Newton–Raphson, and Arc-length technique, to update the stiffness matrix in accordance with changes in the stress–strain relationships and geometries. Peng et al [3] developed a force element method to predict the geometric nonlinear behavior of truss beams. Besides, a higher-order root-solving algorithm was introduced by Maghami et al [4] for large deformation analysis. Moreover, Maghami et al [5] proposed a path-following technique based on the multi-point method. Thanks to its notable advantages, this method has been effectively employed in various nonlinear problems. However, its implementation still demands extensive numerical simulations, which rely heavily on the control parameters of incremental–iterative techniques [5]. To overcome this limitation, an alternative method combining the minimum energy principle with optimization techniques was proposed to directly obtain nonlinear responses without using FEM. To achieve this aim, several gradient-based optimization algorithms were introduced to resolve the above issue. A modified sequential quadratic programming method was formulated by Ohkubo et al [6] to analyze structures through solving the potential or complementary energy minimization problems. Moreover, Toklu [7] introduced an Adaptive Local Search Method (ALSM) to enhance the efficiency of structural analysis. This approach has been successfully implemented for nonlinear structural analysis. Although these methods exhibit relatively fast convergence, they inherently require the explicit evaluation of the derivatives of the energy function with respect to the displacement variables. This dependency significantly increases computational complexity and often becomes a major obstacle in solving practical problems, particularly when the derivative information is difficult or impossible to obtain analytically.

In recent years, gradient-free algorithms have proven highly effective complex optimization problems in which derivative information is unavailable or unreliable. For example, Kaveh and Rahami [8] presented a hybrid approach that combined the force method with a Genetic Algorithm (GA) for nonlinear structural analysis and optimal design. Their results showed that the proposed strategy can efficiently determine both structural responses and optimal member sizes without relying on stiffness-based iterative procedures. Similarly, Toklu et al. [9] introduced a total potential energy optimization method integrated with the Harmony Search (HS) algorithm for nonlinear truss analysis. By minimizing the TPE, the method

© 2026 Trường Đại học Công nghiệp Thành phố Hồ Chí Minh

accurately evaluates structural responses while reducing computational effort. In addition, Temür et al. [10] developed a PSO-based method for geometrically nonlinear truss analysis, in which the equilibrium state is obtained by minimizing the TPE. The proposed approach achieves accurate solutions with strong convergence behavior, without requiring derivative information or stiffness matrix updates. More recently, Bárbara et al. [11] conducted a comprehensive investigation of the performance, efficiency, and accuracy of two metaheuristic algorithms, including the GA and PSO, for the optimum design of truss structures, taking into account both nonlinear behavior and dynamic loading conditions. The mentioned metaheuristic algorithms offer strong global search capabilities, allowing them to effectively handle the highly nonlinear and multimodal nature of structural optimization problems. Furthermore, they do not require derivative information, making them suitable for geometrically nonlinear analyses where analytical gradients are difficult or impossible to obtain. Among gradient-free metaheuristic methods, DE is widely regarded as an efficient and robust algorithm for solving complex continuous optimization problems. Originally introduced by Storn and Price [12], DE is a population-based method that relies on simple yet effective mechanisms of mutation, crossover, and selection to balance exploration and exploitation of the search space. Unlike gradient-based techniques, DE does not require derivative information, making it well suited for nonlinear, non-differentiable, and multimodal problems commonly encountered in structural analysis and optimization. In addition to its simplicity and rapid convergence, DE is known for maintaining population diversity and avoiding premature convergence. Moreover, the algorithm involves only a few control parameters, which facilitates implementation and enables reliable performance across various engineering applications. However, to the best of the authors' knowledge, DE has not yet been applied to the nonlinear analysis of truss structures.

In this paper, a DE-based framework is introduced to conduct geometrically nonlinear analysis of truss structures. In this approach, the TPE is adopted as the objective function to capture the geometrically nonlinear response of the structure. Once the optimization process converges, the structural responses can be obtained directly without performing conventional incremental–iterative analysis. Several numerical case studies are presented to validate the effectiveness of the proposed method. It should be noted that both stiffness-based solvers and metaheuristic approaches are approximate numerical procedures. Accordingly, the proposed method is validated by comparison with well-established benchmark numerical solutions reported in the literature, rather than suggesting that conventional methods provide exact results. The findings confirm that the developed approach is straightforward to implement and capable of delivering highly accurate results.

The paper is organized as follows. Section 2 introduces the formulation of the TPE for truss structures and presents it as an optimization problem. Section 3 describes the DE algorithm used in this study. In Section 4, several benchmark truss examples are analyzed to evaluate the performance and accuracy of the proposed method. Finally, Section 5 summarizes the main conclusions drawn from the numerical results

2 FORMULATION OF THE PROBLEM

Structural analysis determines the equilibrium state of a structure under external loads. In this work, the geometrically nonlinear behavior is formulated by minimizing the TPE of the truss system, denoted as E_T. This energy consists of the strain energy E_s and the external work E_w, and is expressed as follows [9, 10]:

$$E_T = E_s + E_w, \tag{1}$$

where

$$E_s = \sum_{e=1}^{m} A_e L_e e_e, \tag{2}$$

$$E_w = -\mathbf{f}^T \hat{\mathbf{u}}, \tag{3}$$

$$e_e = \int_0^{\varepsilon_e} \sigma_e d\varepsilon_e \tag{4}$$

in which E_e, L_e, and A_e denote the Young's modulus, length, and cross-sectional area of the *e*th truss member, respectively; e_e denotes the strain energy density of the *e*th member; $\hat{\mathbf{u}}$ and $\mathbf{f}$ represent the displacement field and external force; ε_e and σ_e are strain and stress of the *e*th member.

To derive the strain energy density, a space truss element in both the initial and current configurations is considered, as shown in Fig. 1. The coordinates (x_i, y_i, z_i) and (x_j, y_j, z_j) represent the original configuration at the *i*th and *j*th end nodes of the member, respectively. Accordingly, the initial length L_0 of the element is defined as follows:

$$L_0 = \sqrt{(x_j - x_i)^2 + (y_j - y_i)^2 + (z_j - z_i)^2}. \tag{5}$$

Under the action of external loads, the nodal displacements are denoted by (u_i, v_i, w_i) and (u_j, v_j, w_j). Accordingly, the current length L_c of the member can be expressed as follows:

$$L_c = \sqrt{(u_j - u_i + x_j - x_i)^2 + (v_j - v_i + y_j - y_i)^2 + (w_j - w_i + z_j - z_i)^2}. \tag{6}$$

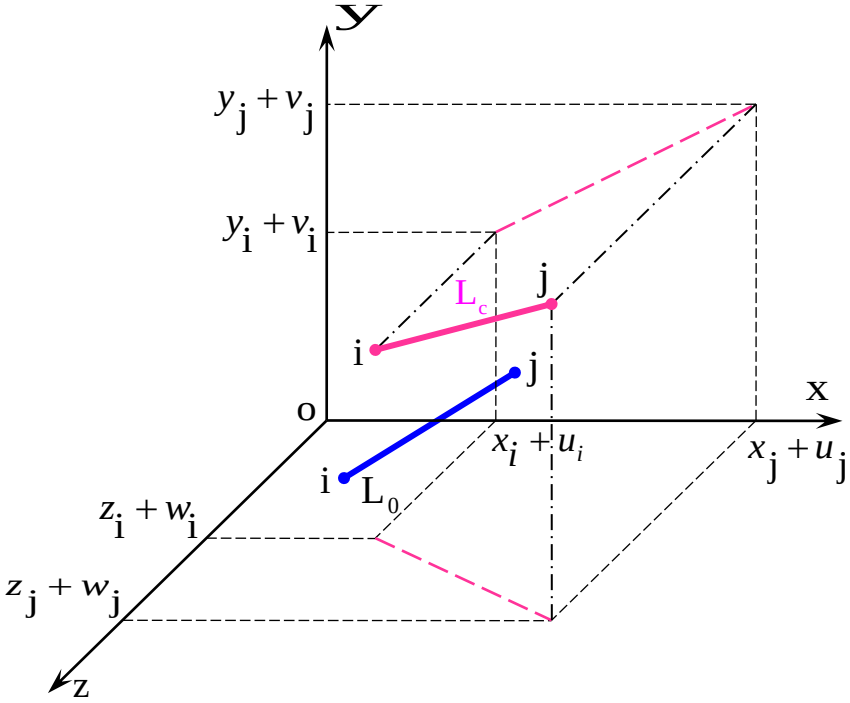


Figure 1: Deformation of a truss member.

It is evident that the axial strain is readily obtained from L_0 and L_c. Several strain measures commonly used in nonlinear structural and solid mechanics are presented below:

Engineering strain: $$\varepsilon_E = \frac{L_c - L_0}{L_0}, \tag{7}$$

Green strain: $$\varepsilon_G = \frac{L_c^2 - L_0^2}{2L_0^2}, \tag{8}$$

Logarithmic strain: $$\varepsilon_L = \log\left(\frac{L_c}{L_0}\right), \tag{9}$$

Almansi strain: $$\varepsilon_A = \frac{L_c^2 - L_0^2}{2L_C^2}, \quad (10)$$

The stress–strain curve $\sigma(\varepsilon)$, which is determined by the material properties, may be linear, piecewise-linear, or nonlinear, and is assumed to be known a priori. Accordingly, once the member-end displacements are known, its strain and strain energy density can be obtained using Eqs. 4 and 7-10.

According to the minimum potential energy principle, the nodal displacement vector $\hat{\mathbf{u}}$ is treated as the primary unknown and is determined by minimizing the total potential energy subject to the prescribed boundary conditions. The general formulation is given as follows:

$$\underset{\hat{\mathbf{u}}}{\text{Minimize}} \qquad E_T(\hat{\mathbf{u}}) = \sum_{e=1}^{m} e_e A_e L_e - \mathbf{f}^T \hat{\mathbf{u}}. \quad (11)$$

When the deflections are treated as design variables, the TPE is adopted as the objective function and minimized using the DE algorithm. Once the displacement field is determined, the internal force in each member is evaluated using the following expression:

$$f_e = A_e \sigma_e(\varepsilon_e), \quad (12)$$

where f_e is the internal force of the eth member.

3 DIFFERENTIAL EVOLUTION

Price and Storn [12] originally proposed the DE algorithm, which has been widely regarded as an effective method for solving optimization problems. In this study, DE is employed as the optimization tool to minimize the TPE of the truss structure. The main steps of the DE algorithm are summarized as follows:

- Initialization

  At the beginning of the optimization process, a random set of n_p individuals is generated within the search space. Each individual corresponds to the ith vector, which contains m design variables $\hat{\mathbf{x}}_i = \{\hat{x}_{i,1}, \ \hat{x}_{i,2}, \ \ldots, \ \hat{x}_{i,m}\}$, and is defined as follows:

  $$\hat{x}_{i,j} = \hat{x}_{min,j} + rand_{i,j}[0,1](\hat{x}_{max,j} - \hat{x}_{min,j}) \quad i = 1,2,\ldots,n_p; \ j = 1,2,\ldots,m, \quad (13)$$

  where $\hat{x}_{min,j}$ and $\hat{x}_{max,j}$ denote lower and upper bounds of $\hat{x}_j$, whereas $rand_{i,j}[0,1]$ represents a uniformly distributed random variable in the range [0, 1]. In the present study, the displacement field is adopted as the design variable.

- Mutation

  In the next step, a mutation operation is applied to the target vector $\hat{\mathbf{x}}_k$ to generate the corresponding mutant vector $\hat{\mathbf{p}}_k$. The two most commonly used mutation strategies are presented below:

  $$\text{best} \ \hat{\mathbf{p}}_i = \hat{\mathbf{x}}_{best} + s(\hat{\mathbf{x}}_{r_1} - \hat{\mathbf{x}}_{r_2}), \quad (14)$$

  $$\text{rand} \ \hat{\mathbf{p}}_i = \hat{\mathbf{x}}_{r_1} + s(\hat{\mathbf{x}}_{r_2} - \hat{\mathbf{x}}_{r_3}), \quad (15)$$

  where r_1, r_2 and r_3 are randomly selected integer indices from $\{1,\ldots,i-1, i+1,\ldots,n_p\}$; s is a scaling factor randomly drawn from the interval (0, 1]; and $\hat{x}_{best}$ denotes the best-performing individual in the population.

Consequently, the mutant vector p_i may violate the prescribed bounds of the design variables. To ensure feasibility, it is adjusted to remain within the allowable limits, as follows:

$$\mathrm{p}_{\mathrm{i,j}} = \begin{cases} 2\hat{\mathrm{x}}_{\mathrm{min,j}} - \mathrm{p}_{\mathrm{i,j}} & \text{if } \mathrm{p}_{\mathrm{i,j}} < \hat{\mathrm{x}}_{\mathrm{min,j}}, \\ 2\hat{\mathrm{x}}_{\mathrm{max,j}} - \mathrm{p}_{\mathrm{i,j}} & \text{if } \mathrm{p}_{\mathrm{i,j}} > \hat{\mathrm{x}}_{\mathrm{max,j}}, \\ \mathrm{p}_{\mathrm{i,j}} & \text{otherwise.} \end{cases} \tag{16}$$

- Crossover

In the third stage, a crossover strategy is employed to maintain population diversity. The trial vector $\mathbf{t}_{\mathrm{i}}$ is then constructed by blending the mutant vector $\mathbf{p}_{\mathrm{i}}$ with its target vector $\hat{\mathbf{x}}_{\mathrm{i}}$, as shown below:

$$\mathrm{t}_{\mathrm{i,j}} = \begin{cases} \mathrm{p}_{\mathrm{i,j}} & \text{if } \mathrm{j} = \ell \text{ or rand } [0,1] \le C_r, \\ \hat{\mathrm{x}}_{\mathrm{i,j}} & \text{otherwise,} \end{cases} \tag{17}$$

In this context, C_r refers to the crossover control parameter, while ℓ denotes a randomly selected integer within the range [1, n_p].

- Selection

At the final stage, the selection strategy is applied to identify the fitter individuals by comparing the objective function values of the trial vectors $\mathrm{f}\left(\mathbf{t}_{\mathrm{i}}\right)$ with those of the corresponding target vectors $\mathrm{f}\left(\hat{\mathbf{x}}_{\mathrm{i}}\right)$ in the population. The selection rule is formulated as follows:

$$\hat{\mathbf{x}}_{\mathrm{i}} = \begin{cases} \mathbf{t}_{\mathrm{i}} & \text{if } \mathrm{f}(\mathbf{t}_{\mathrm{i}}) < \mathrm{f}(\hat{\mathbf{x}}_{\mathrm{i}}) \\ \hat{\mathbf{x}}_{\mathrm{i,j}} & \text{otherwise.} \end{cases} \tag{18}$$

4 NUMERICAL EXAMPLES

This section presents two numerical examples to evaluate the performance of the DE algorithm in the analysis of truss structures. For validation purposes, the obtained results are compared with those produced by the HS and the PSO methods in existing research studies. The DE parameters are configured as follows: crossover factor $C_r = 0.9$, mutation factor $s = 0.8$, population size = 40, maximum number of function evaluations = 9000, and stopping criterion = 10^{-6}. For a fair comparison, the TLBO, BSA, and FA algorithms are implemented using the same population size, maximum number of evaluations, and stopping criterion as the DE algorithm. Due to the stochastic nature of the algorithms, each example is solved thirty times, and the best result is reported. All simulations are implemented in MATLAB on a desktop computer to ensure a fair comparison across methods.

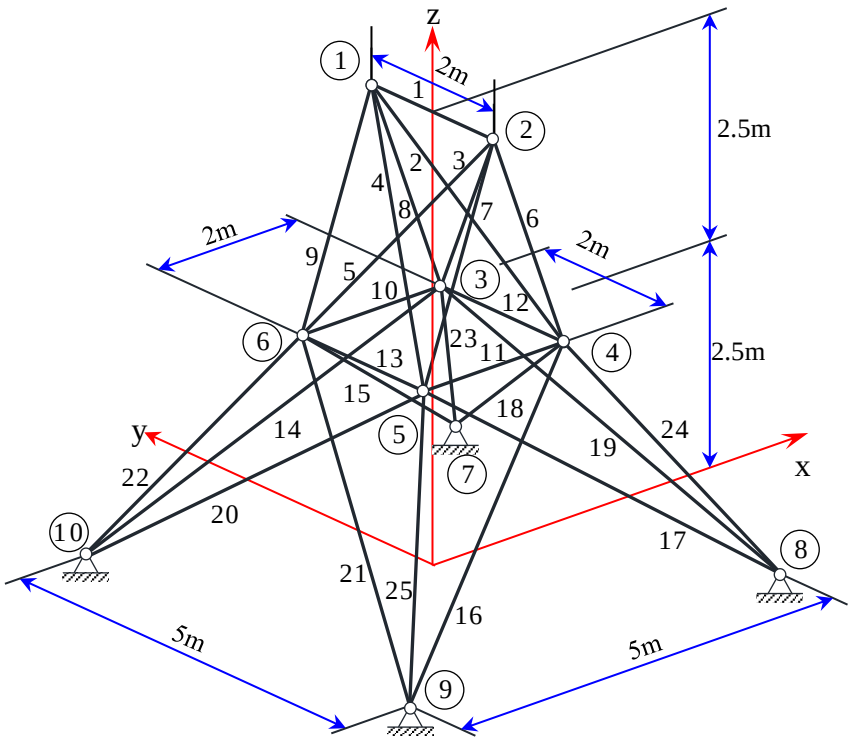


Figure 2: Configuration of the 25-bar spatial truss

4.1 25-bar spatial truss

A 25-member spatial truss, shown in Fig. 2, is analyzed considering the first geometric nonlinearity. All truss elements are modeled with a uniform Young's modulus of 2×10^5N/mm² and a constant cross-sectional area of 10 mm². Three loading conditions, as summarized in Table 1, are examined.

Table 1: Loading scenarios for the geometrically nonlinear 25-bar space truss

Node	Case 1 (kN)			Case 2 (kN)			Case 3 (kN)		
	ox	oy	oz	ox	oy	oz	ox	oy	oz
1	0	80	-20	800	0	-200	800	800	-200
2	0	-80	-20	-800	0	-200	0	0	0

A summary of the comparison between DE and other algorithms under different loading cases is presented in Tables 2-7. In this example, The TPE values obtained by DE show good agreement with those of HS, PSO, BSA, TLBO, and FA for all three loading cases. In the solution quality, the DE demonstrates performance similar to that of the existing algorithms. In terms of computational cost, the proposed framework is more computationally efficient than BSA, TLBO, and FA. In addition, the statistical results including the mean, worst, and best TPEs are reported for comparison. It can be easily seen that the mean TPEs obtained by the DE show a quite good agreement with the best and worst TPEs. Therefore, the obtained results confirm the efficiency and reliability of the proposed model in geometric nonlinear analysis. The errors of the structural responses are less than 0.1% . Besides, the DE requires fewer control parameters than both HS and PSO. The TPE convergence history obtained by the DE for the first loading case is shown in Figure 3. It can be easily seen that the proposed algorithm converges very fast in the early iterations, requiring only 24,360 function evaluations.

Table 2: Comparison of nodal deflections of the 25-bar truss under geometric nonlinearity (Case 1)

Disp No.	PSO [3]	HS [3]	Present

(mm)			BSA	TLBO	FA	DE
u_1	0.06	-0.08	0.00	0.00	-0.08	0.00
v_1	38.01	37.91	37.87	37.92	35.75	37.84
w_1	-37.27	-37.21	-37.21	-37.22	-36.53	-37.20
u_2	0.06	-0.06	0.00	-0.01	0.02	0.00
v_2	-37.68	-37.77	-37.82	-37.78	-36.14	-37.85
w_2	-37.16	-37.15	-37.19	-37.16	-36.71	-37.20
u_3	0.86	0.89	0.87	0.87	0.85	0.87
v_3	-1.73	-1.73	-1.74	-1.74	-1.69	-1.75
w_3	-16.45	-16.34	-16.40	-16.40	-16.25	-16.39
u_4	0.88	0.92	0.86	0.87	0.95	0.87
v_4	1.76	1.75	1.75	1.75	1.71	1.74
w_4	-16.38	-16.36	-16.38	-16.37	-16.46	-16.39
u_5	-0.85	-0.82	-0.87	-0.86	-0.86	-0.87
v_5	1.78	1.75	1.74	1.75	1.58	1.74
w_5	-16.35	-16.40	-16.38	-16.37	-16.37	-16.39
u_6	-0.87	-0.84	-0.87	-0.87	-0.78	-0.87
v_6	-1.70	-1.75	-1.75	-1.74	-1.66	-1.75
w_6	-16.40	-16.43	-16.40	-16.41	-16.43	-16.39
Best TPE (kN.m)	-3.7645	-3.7645	-3.76450	-3.76450	-3.75632	-3.76450
Worst TPE (kN.m)	-	-	-3.76450	-3.76450	-3.75626	-3.76450
Mean TPE (kN.m)	-	-	-3.76450	-3.76450	-3.75628	-3.76450
Number of evaluation	-	-	113560	24400	360000	24360
Total times (s)	-	-	18	8	81	6

Table 3: Comparison of nodal deflections of the 25-bar truss under geometric nonlinearity (Case 2)

Disp No. (mm)	PSO [3]	HS [3]	Present			
			BSA	TLBO	FA	DE
u_1	1260.63	1257.53	1260.76	1260.34	493.41	1261.069
v_1	-529.80	-527.51	-530.78	-529.87	-419.40	-528.798
w_1	-455.35	-455.55	-456.03	-455.79	-295.30	-456.629
u_2	-1261.15	-1264.62	-1261.36	-1261.60	-1110.35	-1261.014
v_2	529.20	529.74	526.89	528.22	-121.86	528.623
w_2	-455.38	-457.91	-457.01	-456.54	-206.33	-456.740
u_3	-47.50	-48.86	-48.44	-47.88	-361.00	-48.678
v_3	-287.03	-288.34	-287.80	-287.29	-581.72	-288.316
w_3	-361.33	-362.12	-362.02	-361.78	-407.58	-362.771

u_4	-203.19	-203.11	-202.83	-203.14	-501.79	-202.695
v_4	-295.57	-296.62	-296.59	-295.96	-665.55	-296.836
w_4	-68.84	-67.54	-69.34	-68.98	-22.78	-68.405
u_5	47.10	48.77	48.38	47.69	404.16	48.727
v_5	286.57	288.71	288.32	287.53	758.69	288.391
w_5	-361.26	-363.58	-363.04	-362.16	-752.94	-362.861
u_6	202.95	202.23	202.73	202.91	-139.75	202.752
v_6	295.18	297.26	296.54	296.09	81.79	296.885
w_6	-68.67	-69.19	-67.73	-68.44	128.92	-68.403
Best TPE (kN.m)	-1444.60	-1444.60	-1444.57126	-1444.57088	-664.06652	-1444.57152
Worst TPE (kN.m)	-	-	-1444.57123	-1444.57085	-664.06079	-1444.57149
Mean TPE (kN.m)	-	-	-1444.57125	-1444.57086	-664.06198	-1444.57151
Number of evaluation	-	-	215160	35320	360000	28200
Total times (s)	-	-	51	17	89	7

Table 4: Comparison of nodal deflections of the 25-bar truss under geometric nonlinearity (Case 3)

Disp No. (mm)	PSO [3]	HS [3]	Present		
			BSA	TLBO	DE
u_1	2521.86	2522.41	2522.81	2522.67	2523.01
v_1	1839.88	1840.28	1840.43	1840.59	1840.92
w_1	-3076.40	-3078.90	-3082.76	-3081.88	-3083.25
u_2	2435.57	2437.30	2440.91	2440.74	2441.43
v_2	2522.31	2522.97	2522.64	2522.42	2523.07
w_2	-1433.56	-1435.86	-1441.17	-1440.45	-1441.90
u_3	-393.83	-393.94	-394.65	-394.71	-394.56
v_3	-371.22	-371.21	-371.53	-371.52	-371.32
w_3	-903.69	-904.68	-905.30	-904.66	-905.31
u_4	579.02	579.07	578.88	578.68	579.04
v_4	198.35	198.93	198.78	198.74	199.13
w_4	45.45	44.97	44.46	44.75	44.45
u_5	1012.54	1013.81	1014.96	1014.85	1015.44
v_5	1036.29	1037.33	1038.08	1038.05	1038.58
w_5	-351.08	-353.07	-355.64	-355.36	-356.42
u_6	406.51	407.35	408.17	407.97	408.38
v_6	802.21	802.64	802.75	802.76	803.11
w_6	-36.68	-36.62	-36.60	-36.35	-36.74
Best TPE (kN.m)	-2860.50	-2860.50	-2860.48547	-2860.48513	-2860.48566
Worst TPE (kN.m)	-	-	-2860.48538	-2860.48507	-2860.48560

Mean TPE (kN.m)	-	-	-2860.48544	-2860.48510	-2860.48563
Number of evaluation	-	-	182800	39560	27520
Total times (s)	-	-	43	15	7

Table 5: Comparison of internal forces for the 25-bar truss under geometric nonlinearity (Case 1)

Forces (kN)	PSO [3]	HS [3]	Present			
			BSA	TLBO	FA	DE
f_1	75.690	75.676	75.696	75.691	71.891	75.693
f_2	3.902	3.915	3.892	3.899	3.495	3.894
f_3	3.869	3.883	3.894	3.891	3.442	3.893
f_4	3.898	3.890	3.895	3.897	3.466	3.893
f_5	3.881	3.885	3.894	3.891	3.525	3.893
f_6	-13.879	-13.844	-13.882	-13.873	-13.506	-13.882
f_7	-13.874	-13.875	-13.882	-13.876	-13.578	-13.884
f_8	-13.909	-13.899	-13.885	-13.889	-13.532	-13.884
f_9	-13.907	-13.894	-13.885	-13.887	-13.469	-13.884
f_{10}	1.730	1.736	1.735	1.734	1.637	1.731
f_{11}	1.730	1.745	1.733	1.731	1.806	1.735
f_{12}	-3.490	-3.482	-3.490	-3.486	-3.400	-3.489
f_{13}	-3.480	-3.497	-3.486	-3.490	-3.239	-3.488
f_{14}	-3.413	-3.376	-3.396	-3.398	-3.373	-3.395
f_{15}	-3.402	-3.412	-3.397	-3.399	-3.444	-3.395
f_{16}	-3.385	-3.366	-3.394	-3.389	-3.388	-3.395
f_{17}	-3.385	-3.412	-3.391	-3.390	-3.418	-3.394
f_{18}	-4.660	-4.657	-4.654	-4.651	-4.673	-4.656
f_{19}	-4.664	-4.643	-4.657	-4.656	-4.599	-4.656
f_{20}	-4.656	-4.654	-4.652	-4.653	-4.594	-4.655
f_{21}	-4.643	-4.662	-4.659	-4.658	-4.625	-4.656
f_{22}	-7.385	-7.378	-7.372	-7.376	-7.383	-7.366
f_{23}	-7.397	-7.355	-7.371	-7.373	-7.312	-7.365
f_{24}	-7.361	-7.365	-7.361	-7.356	-7.429	-7.368
f_{25}	-7.333	-7.358	-7.364	-7.355	-7.404	-7.367

Table 6: Comparison of internal forces for the 25-bar truss under geometric nonlinearity (Case 2)

Forces (kN)	PSO [3]	HS [3]	Present			
			BSA	TLBO	FA	DE
f_1	691.627	692.590	692.410	692.098	340.581	692.4635
f_2	-334.677	-334.408	-334.767	-334.722	-113.737	-334.5996

f_3	73.231	73.046	72.980	73.218	127.411	72.7267
f_4	73.245	72.343	72.711	72.894	-57.754	72.7612
f_5	-334.761	-334.711	-334.438	-334.532	-157.962	-334.5660
f_6	275.049	275.294	274.606	274.773	133.345	274.5598
f_7	-189.519	-189.137	-189.408	-189.590	386.391	-189.2164
f_8	-189.291	-189.279	-189.162	-189.281	-52.897	-189.1830
f_9	275.003	273.927	274.810	274.720	-3.136	274.6589
f_{10}	-132.998	-132.535	-132.788	-132.888	-27.165	-132.7537
f_{11}	-132.948	-132.868	-132.743	-132.913	-61.309	-132.7243
f_{12}	35.618	35.618	35.860	35.826	123.726	35.8105
f_{13}	35.781	35.798	35.678	35.844	-319.482	35.7988
f_{14}	-51.883	-52.294	-52.226	-52.073	-108.223	-52.3751
f_{15}	-125.189	-125.339	-125.054	-125.238	67.317	-125.2729
f_{16}	-125.368	-125.143	-125.495	-125.434	-253.557	-125.2481
f_{17}	-51.825	-52.509	-52.331	-52.048	-150.840	-52.3979
f_{18}	115.587	116.226	115.773	115.684	302.249	116.0448
f_{19}	-174.273	-174.651	-174.512	-174.378	-224.241	-174.8179
f_{20}	-174.273	-174.651	-174.927	-174.575	-345.924	-174.8556
f_{21}	115.450	115.946	116.095	115.811	40.115	116.0711
f_{22}	-45.834	-46.776	-45.778	-45.942	2.119	-46.1589
f_{23}	-55.429	-54.925	-55.194	-55.436	128.442	-55.2539
f_{24}	-45.918	-45.581	-46.500	-46.089	8.365	-46.1674
f_{25}	-55.700	-55.421	-55.452	-55.566	93.596	-55.2507

Table 7: Comparison of internal forces for the 25-bar truss under geometric nonlinearity (Case 3)

Forces (kN)	PSO [3]	HS [3]	Present		
			BSA	TLBO	DE
f_1	107.691	107.640	106.678	106.791	106.522
f_2	273.432	273.603	274.187	274.251	274.317
f_3	-310.660	-310.372	-310.645	-310.697	-310.738
f_4	247.501	247.023	246.502	246.551	246.378
f_5	-70.574	-70.532	-70.033	-69.905	-69.980
f_6	-10.110	-10.172	-10.737	-10.724	-10.805
f_7	359.219	359.301	359.410	359.455	359.426
f_8	186.599	187.014	187.550	187.612	187.715
f_9	471.760	471.844	472.028	472.029	472.098
f_{10}	-111.052	-110.993	-111.399	-111.490	-111.434

f_{11}	-179.696	-180.275	-180.560	-180.632	-180.606
f_{12}	-26.821	-26.908	-26.722	-26.920	-26.794
f_{13}	-106.819	-106.789	-106.848	-106.785	-106.771
f_{14}	-260.427	-260.641	-260.931	-260.840	-260.945
f_{15}	-236.904	-237.250	-237.532	-237.398	-237.666
f_{16}	238.851	238.850	238.649	238.636	238.753
f_{17}	-177.046	-177.597	-178.280	-178.197	-178.452
f_{18}	-125.457	-125.783	-125.849	-125.739	-125.988
f_{19}	-247.944	-248.091	-248.164	-248.036	-248.112
f_{20}	-189.732	-190.078	-190.556	-190.511	-190.735
f_{21}	332.074	332.335	332.509	332.531	332.643
f_{22}	-52.744	-52.549	-52.255	-52.211	-52.292
f_{23}	-106.436	-106.707	-106.520	-106.301	-106.638
f_{24}	-50.697	-50.752	-51.014	-50.853	-50.934
f_{25}	541.876	542.045	541.940	541.978	542.056

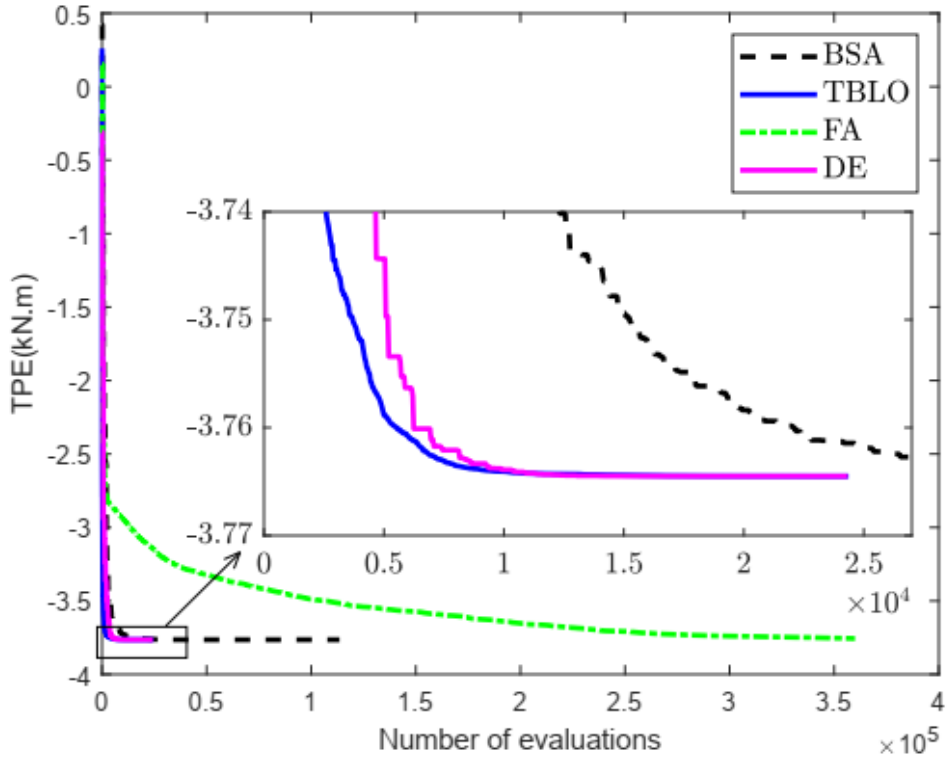


Figure 3: The TPE convergence histories of the 25-bar spatial truss(Case 1)

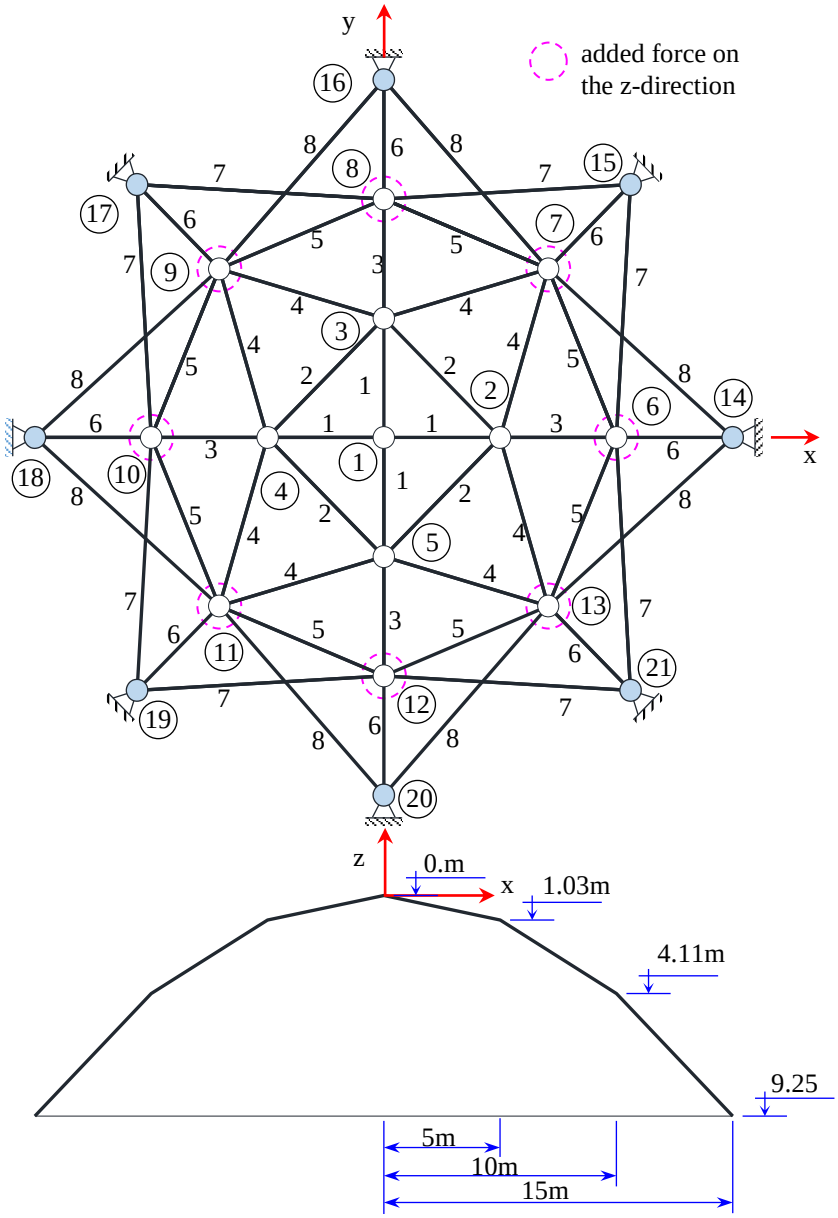


Figure 4: 52-bar dome truss.

4.2 52-bar dome truss

A 52-bar dome truss, illustrated in Fig. 4, is considered for the subsequent geometrically nonlinear analysis. The optimal cross-sectional areas of the members, reported by Mai et al. [13], are adopted in this study. The truss members are divided into eight groups with the following areas: $A_1 = A_2 = A_3 = A_4 = A_8 = 2$ cm², $A_5 = 16.672$ cm², $A_6 = 17.585$ cm², and $A_7 = 2.519$ cm². All elements are assumed to be made of a linearly elastic material with a Young's modulus of E = 21,000 kN/cm². The structure is subjected to a vertical concentrated load of $P_z = 150$ kN, applied at nodes 6 through 13.

Similar to the 25-bar space truss discussed earlier, Tables 8-9 present a comparison between the results obtained using the DE algorithm and those from other algorithms. It can be observed that DE provides highly accurate estimates of the structural response corresponding to the minimum TPE value. Moreover, this method exhibits superior computational efficiency, especially as the structural complexity increases. In particular, the mean error of the DE algorithm relative to FEM is less than 0.35%. Furthermore, the mean, worst, and best TPE values are very close, indicating that the DE algorithm exhibits stability and consistent

convergence across multiple runs, with low sensitivity to stochastic initialization. In addition, its computational overhead is approximately 50% lower than that of the other methods. Fig. 5 illustrates the convergence history of the TPE obtained by the DE and the optimal solution is found after 126,880 function evaluations.

Table 8: Comparison of displacements (mm) for the 52-bar dome truss

Deflections (mm)	Mai [13]	FEM	Present			
			BSA	TLBO	FA	DE
w_1	1.328	1.328	1.339	1.322	1.338	1.325
w_2	0.720	0.720	0.671	0.720	0.717	0.724
w_6	10	10.009	10.027	10.031	9.981	10.005
w_7	10	10.008	9.903	9.937	10.017	9.995
Best TPE (kN.cm)	-	-599.369	-599.3412	-599.3468	-599.3327	-599.3492
Worst TPE (kN.cm)	-	-	-599.3409	-599.3468	-599.3320	-599.3492
Mean TPE (kN.cm)	-	-	-599.3410	-599.3468	-599.3322	-599.3492
Number of evaluation	-	-	360000	192520	360000	126880
Total times (s)	-	-	162	127	167	59

Table 9: Comparison of member forces in the geometrically nonlinear 52-bar truss

Force (N)	Connection	FEM	Present			
			BSA	TLBO	FA	DE
f_1	1-2	0.000	-0.064	-0.036	0.090	-0.022
f_5	2-3	1.051	1.048	1.029	0.988	1.055
f_9	2-6	2.981	2.806	2.810	3.137	2.969
f_{12}	2-7	2.981	3.201	2.908	2.802	2.965
f_{21}	6-7	-174.849	-174.682	-174.566	-174.622	-174.704
f_{29}	6-14	-185.263	-185.224	-185.113	-184.958	-185.108
f_{30}	7-15	-194.176	-194.099	-194.006	-193.744	-194.017
f_{37}	6-15	-18.338	-18.507	-18.406	-18.337	-18.340
f_{45}	7-14	-14.604	-14.454	-14.517	-14.559	-14.581

5 CONCLUSIONS

In this study, a differential evolution-based approach is proposed to address the geometric nonlinearity in truss structures. The displacement field is obtained by minimizing the system's total potential energy, which serves as the objective function of the DE algorithm. The efficiency and practicality of the method are demonstrated through two benchmark truss problems. Results show that DE achieves the TPE values in good agreement with those obtained by alternative algorithms. Notably, this approach is capable of finding solutions without performing conventional structural analyses. Owing to these advantages, it offers a promising framework for solving nonlinear structural problems without relying on incremental-iterative techniques.

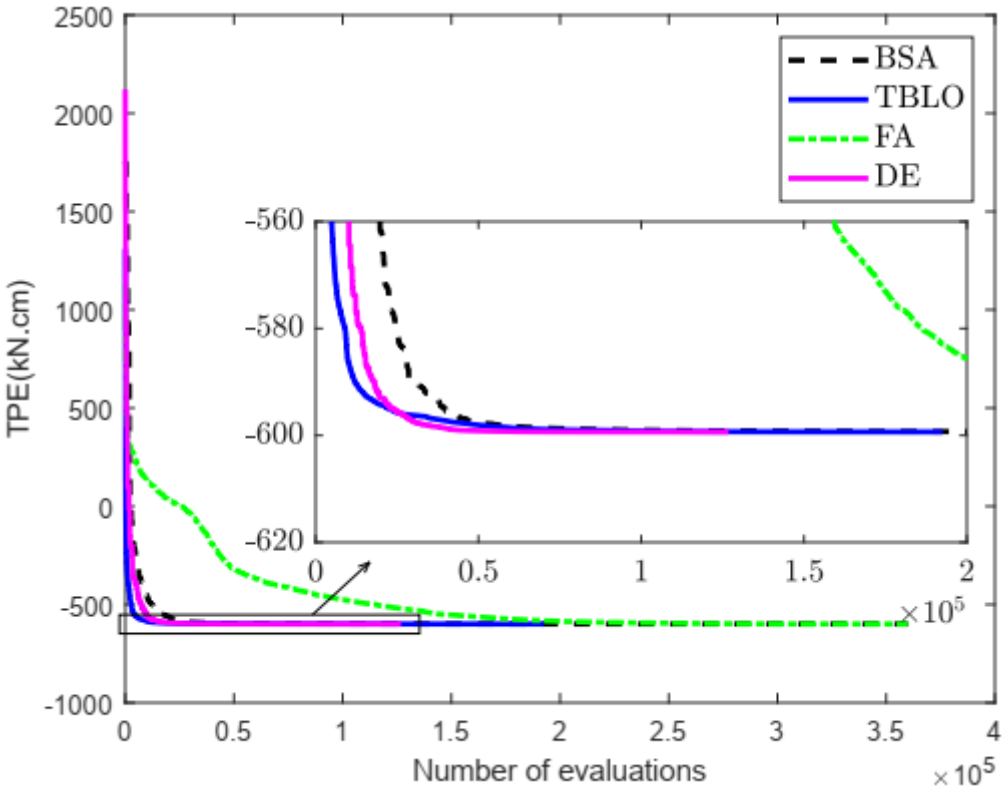


Figure 5: The TPE convergence history of the 52-bar dome truss

REFERENCES

[1] P. Mata, S. Oller, A. Barbat, Static analysis of beam structures under nonlinear geometric and constitutive behavior, *Computer methods in applied mechanics and engineering*, vol. 196, no. 45-48, pp. 4458–4478, 2007.

[2] M. Greco, F. Gesualdo, W. Venturini, H. Coda, Nonlinear positional formulation for space truss analysis, *Finite Elements in Analysis and Design*, vol. 42, no. 12, pp. 1079–1086, 2006.

[3] Y. Peng, Z. Li, M.M. Kamel, Geometrical nonlinear problems of truss beam by base force element method, *International Journal for Numerical Methods in Engineering*, vol. 122, no. 18, pp. 4793–4824, 2021.

[4] [12] A. Maghami, F. Shahabian, S.M. Hosseini, Geometrically nonlinear analysis of structures using various higher order solution methods: a comparative analysis for large deformation, *Computer Modeling in Engineering & Sciences*, vol. 121, no. , pp. 877–907, 2019.

[5] A. Maghami, F. Shahabian, S.M. Hosseini, Path following techniques for geometrically nonlinear structures based on multi-point methods, *Computers & Structures*, vol. 208, pp. 130–142, 2018.

[6] S. Ohkubo, Y. Watada, F. Toshio, Nonlinear analysis of truss by energy minimization, *Computers & Structures*, vol. 27, pp. 129–145, 1987.

[7] Y. Toklu, Nonlinear analysis of trusses through energy minimization, *Computers & Structures*, vol. 82, pp. 1581–1589, 2004.

[8] A. Kaveh, H. Rahami, Nonlinear analysis and optimal design of structures via force method and genetic algorithm, *Computers & Structures*, vol. 84, pp. 770–778, 2006.

[9] Y.C. Toklu, G. Bekda ̧s, R. Temur, Analysis of trusses by total potential optimization method coupled with harmony search, *Structural Engineering and Mechanics*, vol. 45, pp. 183–199, 2013.

[10] R. Temür, Y.S. Türkan, Y.C. Toklu, Geometrically nonlinear analysis of trusses using particle swarm optimization, *Recent Advances in Swarm Intelligence and Evolutionary Computation*, vol. 585, pp. 283–300, 2015.

[11] Domingues, Bárbara Scardini, Marcos Antônio Campos Rodrigues, and Élcio Cassimiro Alves, Optimum Design of truss structures considering nonlinear analysis and dynamic loading using metaheuristic algorithms, *REM-International Engineering Journal*, vol. 78, no. 1 , 2025.

[12] Price, Kenneth V., Rainer M. Storn, and Jouni A. Lampinen, Differential evolution: a practical approach to global optimization, *Springer Berlin Heidelberg*, pp. 37–134, 2005.

[13] Mai, Hau T., Joowon Kang, and Jaehong Lee, A machine learning-based surrogate model for optimization of truss structures with geometrically nonlinear behavior, *Finite Elements in Analysis and Design*, vol. 196, pp. 103572, 2021.

MÔ HÌNH DỰA TRÊN THUYẾT TIẾN HÓA CHO PHÂN TÍCH PHI TUYẾN HÌNH HỌC CẤU TRÚC THANH

MAI TIẾN HẬU

Khoa Công nghệ Cơ khí, Đại học Công nghiệp Thành phố Hồ Chí Minh

Tác giả liên hệ: maitienhau@iuh.edu.vn

Tóm tắt. Nghiên cứu này trình bày phương pháp tối thiểu hóa năng lượng dựa trên thuật toán tiến hóa (DE) cho bài toán phân tích phi tuyến hình học kết cấu dàn. Trạng thái cân bằng của kết cấu được xác định bằng cách tối thiểu hóa năng lượng thế năng sử dụng DE, qua đó tránh được việc cập nhật độ cứng và các bộ giải gia tải. Giải thuật DE không cần đạo hàm và có ít tham số điều khiển, cung cấp khả năng tìm kiếm toàn cục mạnh mẽ trong các bài toán phi tuyến. Trong phương pháp này, trường chuyển vị được xem như các biến thiết kế, và các đáp ứng phi tuyến của kết cấu được xác định thông qua việc tối thiểu hóa trực tiếp phiếm hàm năng lượng mà không cần tính ma trận độ cứng tiếp tuyến hoặc đánh giá đạo hàm. Hiệu năng của khung phương pháp đề xuất được đánh giá thông qua một số ví dụ số và kết quả đạt được so sánh với các công bố trước đó và cácthuật toán tối ưu hóa khác như TLBO, FA, và BSA. Kết quả cho thấy phương pháp đề xuất có khả năng xác định chính xác trạng thái cân bằng của kết cấu.

Từ khóa. Phân tích phi tuyến; Cấu trúc thanh; Tính phi tuyến hình học; Thuật toán tiến hóa.

Ngày gửi bài: 09/11/2025
Ngày chấp nhận đăng:18/12/2025